Frontiers in Materials Technologies, edited by M.A. Meyers and O.T. Inal
Elsevier Science Publishers B.V., 1985 — Printed in The Netherlands

CHAPTER 1

DEVELOPMENTS AND PROSPECTS IN MATERIALS TECHNOLOGIES

Marc A. Meyers
Osman T. Inal

Department of Metallurgical and Materials Engineering
and Center for Explosives Technology Research
New Mexico Institute of Mining and Technology
Socorro, New Mexico 87801

I. INTRODUCTION

Materials have been traditionally divided into three groups: metals, ceramics, and polymers. This classification has its origin in the nature of the interatomic bonding, which ultimately determines the properties. These three classes of materials were studied, produced, and utilized by metallurgists, ceramists, and polymer chemists, respectively. With the emergence of the field of materials science and engineering, in the 60's, a new educational approach was implemented, emphasizing the fundamental study of the structure, properties, and processing of materials. Concomitantly with the unification of their study, the broadening of the boundaries of each class of materials took place. If one looks at the field of materials today, one can see a spectrum of structures and properties that is approaching a continuum. The old statements

*metals are crystalline

*polymers are insulators

*ceramics are brittle

have lost their meaning; non-crystalline metals have been developed and present a bright technological potential (Chapter 5); conductive polymers exist today and have unique properties and applications (Chapter 10); the addition of second phases has dramatically increased the ductility of cement (Chapter 7) and stress-induced transformations have resulted in partially-stabilized zirconia with a fracture toughness of ~8 $MN/m^{3/2}$ (Chapter 8). A new group of materials -- composites -- consists of mixtures of two or more classes (Chapters 6 and 12). In order to arrive at this wide spectrum of properties, new processing techniques had to be developed. For most cases, these have been successful only after large development programs addressing both the processing and properties of the

materials. Cohen et alii (1) proposed a core for Materials Science and Engineering consisting of a structure-property-performance triangle in wich each of the three parameters is dependent on the other two; the three are affected by processing. The increasing complexity of the interplay between societal needs and scientific findings in a technologically advanced society is still not completely understood. What is understood are the ingredients required for technological innovation in materials: (a) scientific discoveries; (b) development programs involving large groups of scientists and engineers; (c) existance of application for product or generation of a new application; (d) economic feasibility or cost competitiveness.

The purpose of this chapter is (a) to complement the material presented in the other chapters and (b) to describe some of the relevant work done by the authors. No attempt is made here to comprehensively review all technologies having a bright potential. The choice was biased by personal experience and is an attempt to provide descriptions of areas not covered by the various chapters.

II. CERAMICS

Three ceramic compounds are being presently developed to play a major role in the significant changes taking place in automotive engines. The "ceramic engine" is in the plans of many automobile manufacturers. Silicon nitride (Si_3N_4), silicon carbide (SiC), and partially stablized zirconia (PSZ) are the principal candidates. Figure 1 shows the effect of temperature on the strength of these ceramics. Partially stablized zirconium oxide contains additions of Y_2O_3 and MgO which stabilize most of the zirconia into the cubic structure. Small pockets of unstable material in the tetragonal phase are retained in the structure. When a crack propagates through zirconia, the tetragonal phase transforms to cubic, with a volume expansion that decreases the stress concentration. The indentation fracture toughness of PSZ is $8 MNm^{-3/2}$ while those of Si_3N_4 and SiC are 4.6 and 3.6 $MNm^{-3/2}$, respectively (2). One problem with PSZ is that the strength decreases significantly with temperature.

Silicon nitride is fabricated by hot pressing, hot isostatic pressing, sintering, or by reaction binding. Hot pressing and hot isostatic pressing, produced by the simultaneous application of pressure and heat, result in the strongest parts. However, net shape capability is limited. Therefore, pressing and sintering seems to present the best balance between mechanical strength and the ability to be formed into complex shapes. Silicon carbide is produced by the same techniques as silicon nitride. Its advantage is the high-temperature strength, although the room temperature strength is lower than that of SiC; it is maintained virtually unchanged up to 1400°C as shown in Figure 1.

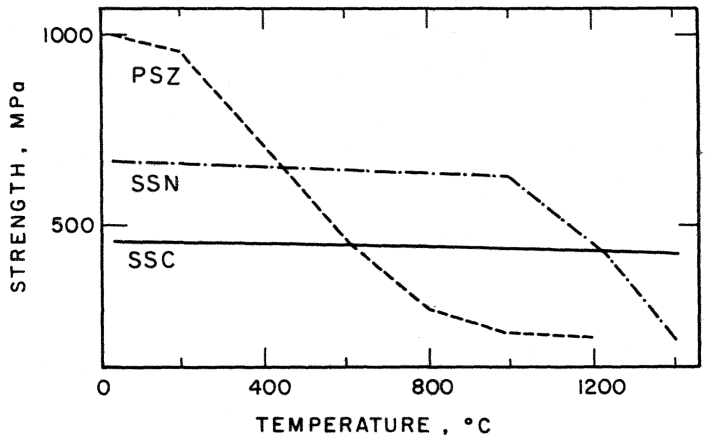

FIGURE 1. Effect of temperature on strength of silicon carbide (SSC), silicon nitride (SSN), and partially stabilized zirconia (PSZ). (Adapted from (1), p. 40).

At least three different design concepts are being developed for the application of ceramics in engines. The application closest to actual production is in turbo-chargers. These turbo-chargers have speeds of up to 100,000 rpm and can be made of SiC and Si_3N_4. The diesel engine with ceramic components shown in Figure 2 is another objective. The ceramic components are crosshatched. This engine would operate at much higher temperatures than present-day engines. No lubricant would be needed, and the utilization of the low thermal conductivity of Si_3N_4 or PSZ would greatly decrease heat losses and the need for a coolant circuit. In this "adiabatic" engine the exhaust gases are much hotter than in conventional diesel engines. These gases are used to drive a turbocharger that is linked to the transmission to generate extra power. In the more distant future, one can envisage the automotive gas turbine operating at temperatures up to 1360°C. This temperature is above the capability of superalloys and ceramics would be required.

Although ceramics are by no means the only materials used in implants--alloys such as Vitalliumand polymers have been proven highly successful--their applications are noteworthy. Biocompatibility is a major concern in all implants, and ceramics are especially attractive because of their chemical inertness. Porous alumina ceramics have been utilized in bone implants, and bone regrowth and bonding are enhanced by the porosity. Alumina is bioinert and is an excellent material for roots in dental applications. Figure 3 shows several posts manufactured of of single-crystal alumina (3). These posts are implanted in the jaw bone and have shown excellent results. Alumina has also been successfully used as a filler to replace parts of bone removed. Tricalcium phosphate (TCP) is undergoing

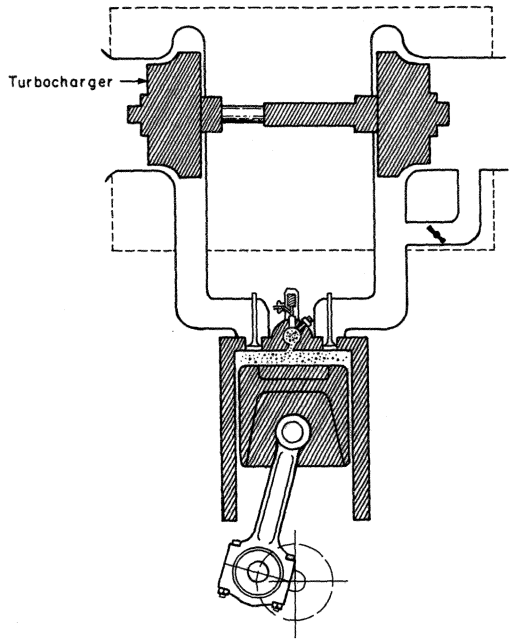

FIGURE 2. The ceramic engine; ceramic components are hatched (Adapted from J.C. Bittence, Materials Engineering, August (1978) 18, p. 20).

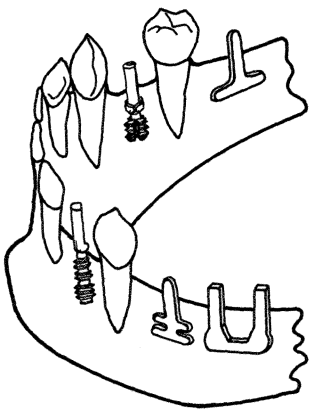

FIGURE 3. Different configurations of ceramic dental implants (Adapted from (3), p. 38).

extensive research in both the porous and densified conditions. The ceramic-bone interface shows excellent strength, evidence of biocompatibility. Porosity allows bone ingrowth which enhances bonding; however, strength is decreased. Multicomponent systems consisting of alumina and spinel are being used to manufacture tooth crowns. These crowns are much stronger than the conventional procelain ones used for the anterior teeth and have been successfully used for the posterior teeth. The compressive strength of these alumina-spinel crowns is of the order of 1,050 MPa (150,000 psi), compared with 350 MPa (50,000 psi) for the natural human teeth.

III. RAPID SOLIDIFICATION

A. General Comments

The splat-cooling experiments conducted by Duwez and coworkers (4,5) in 1960 have triggered a new technological cycle within metallurgy. By cooling metals from the liquid state at rates of the order of 10,000°C/sec or higher, a whole range of new microstructures has been made possible. The principal characteristics obtainable by rapid solidification are:

a) Extended solid solutions; the solubility limits can be exceeded considerably without phase separation because of the fast cooling rate.

b) Refinement of precipitates; massive second-phase particles (such as MC carbides in superalloys) that embrittle the alloys are eliminated by the rapid cooling rate; they may be replaced by very fine distributions of precipitates.

c) Microcrystalline and microdendritic structures; as the cooling rate is increased, the dendrite arm spacing decreases during solidification. At a critical cooling rate the microdendritic structure changes to microcrystalline. This microcrystalline structure is characterized by micrograins ($<1\mu m$) separated by large angle grain boundaries.

d) Metastable crystalline phases; the rapid cooling rates can create a whole range of non-equilibrium crystalline structures; diffusion is virtually eliminated by rapid solidification.

e) Metallic glasses (or non-crystalline metals); beyond a certain cooling rate the crystalline structure does not have time for nucleation and growth. Hence, the liquid structure (non-crystalline) is retained.

Figure 4 shows the effect of increasing the cooling rate on the solidification microstructure. Intense research activity exists presently in the field of rapid solidification technology. In Chapter 5 Gilman describes all aspects of metallic glasses, while in Chapter 4 Grant presents the rapid solidification technology applied to aluminum-lithium alloys.

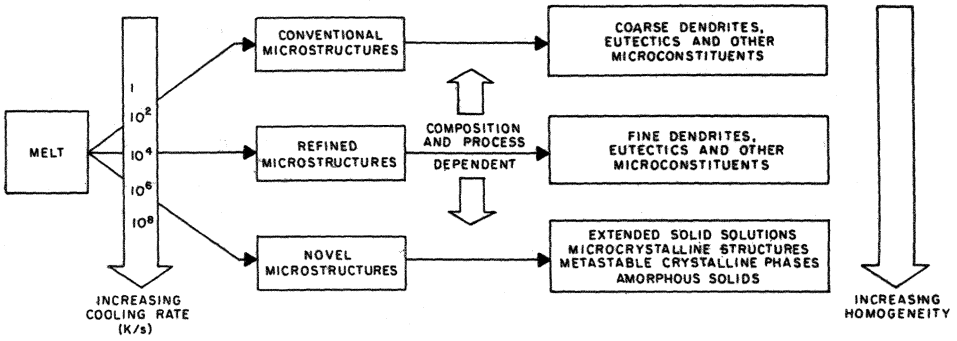

FIGURE 4. Effect of solidication rate on microstructure (From (1)).

Figure 5 shows MarM-200 and IN-100 particles produced by the Pratt and Whitney RSR (rapid solidification rate) process. The powders produced by this method are close to spherical in shape. While the microdendritic structure of MarM-200 can be clearly seen on the surface of the particle and in the photomicrograph of the cross-section, IN-100 exhibits a microcrystalline structure.

A number of different techniques have been developed to produce the rapidly-solidified alloys. Savage and Froes (6) describe these production techniques. Some of these methods are shown in Figure 6. In inert gas atomization a liquid jet is made to produce small droplets, which are cooled by gas jets. The centrifugal atomization process uses a rotating disk on which the liquid stream impinges. The fine liquid layer formed separates into small particles. The Pratt and Whitney RSR process is based on this concept. Melt spinning is the technique used for the production of metallic glass ribbons. The liquid metal solidifies when it enters in contact with the rotating copper drum and a continuous strip is formed by this method. In melt extraction, the rotating disk extracts the liquid from the surface. The rotating electrode technique uses an electric arc generated by a high voltage to melt the surface of the electrode; its rotation imparts a kinetic energy to the particles, which separate.

The production of the rapidly solidified powders/ribbons/slivers is only the first processing stage. Consolidation into a three-dimensional shape is an important step, and several techniques have been developed. Hot isostatic pressing (HIP) followed by forging seems to be the most effective method for superalloy powders. In hot isostatic pressing (this technique is also applied to casting, in order to "heal" their defects, as shown in Section V) the powders are loaded into a can having dimensions that are somewhat higher than the final part

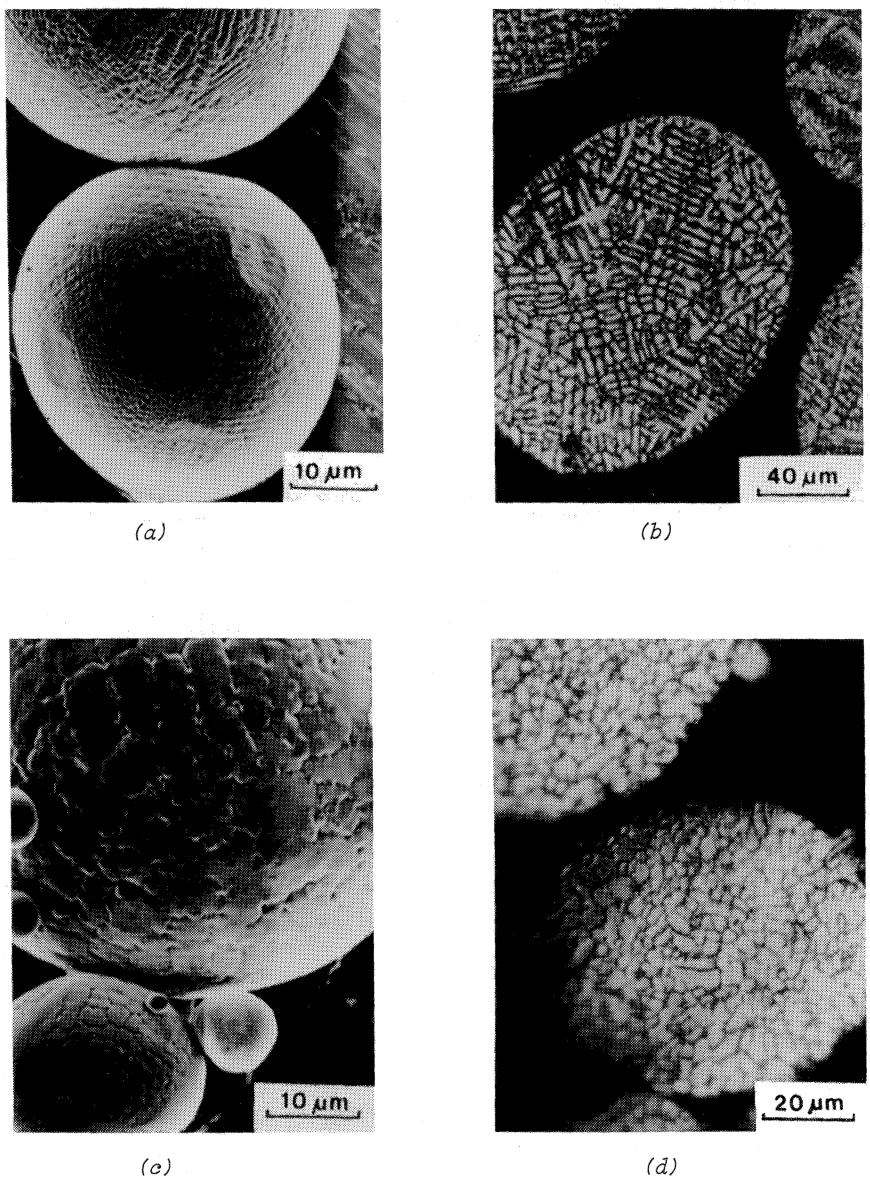

(a) (b)

(c) (d)

FIGURE 5. Rapidly-solidified particles. (a) and (b) SEM and optical micrograph of cross-section of RSR MarM-200 showing microdendrites. (c) and (d) SEM and optical micrograph of cross-section of RSR IN-100 showing micrograins. (Specimens courtesy of Pratt and Whitney).

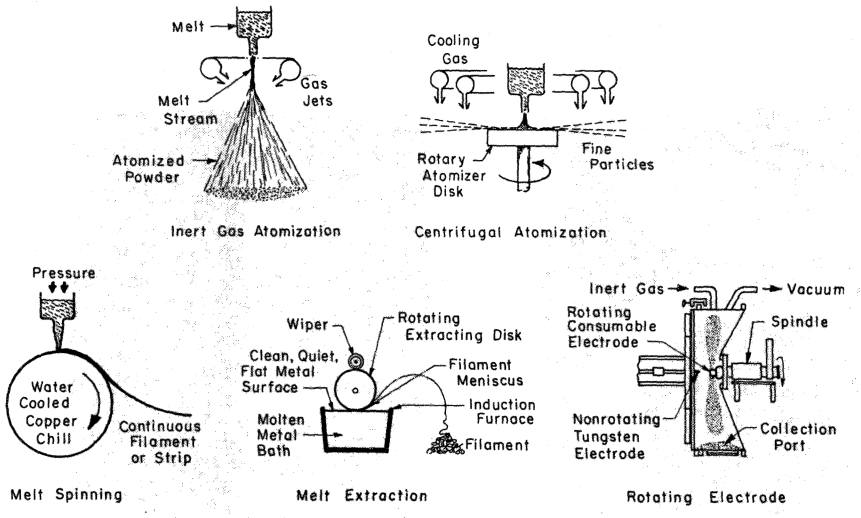

FIGURE 6. Most common processes for producing rapidly-solidified powders and ribbons.

(Figure 7(a)). The can is then outgassed and sealed, after evacuation. The cans are placed in a furnace under a pressure applied by a gas, for a specified temperature and time. The external pressure promotes the sintering of the particles, with the elimination of the interparticle voids (Figure 7(c)). After this, the product is decanned, forged, and heat treated.

The small grain size in some superalloy powders makes them behave superplastically, at a controlled temperature and strain rate. Some superalloys are processed by the Pratt and Whitney "Gatorizing" process. It consists of hot extrusion of the canned powder. Recrystallization takes place during extrusion, leading to a very small grain size. This fine-grained material can then be processed (forged) superplastically at a low strain rate. For example, IN-100 with a grain size of 10 μm can undergo a total elongation of 1,000 pct.

Powder rolling is another attractive technique leading directly from the powder to sheet material (7). In Figure 8 the process is schematically shown. Blended powder is fed from a hopper to the space between two rolls. The high pressure distorts the particles and forces them into intimate contact. This green compact has sufficient strength for handling; it is then sintered in a furnace under an atmosphere that inhibits oxidation.

B. Non-Crystalline Alloys

Structural characterization of amorphous alloys indicates that, in general, no periodicity exists in the atomic arrangement of these materials (as shown in Figure 9(a-d)) and that there are only weak correlations in the atomic positions

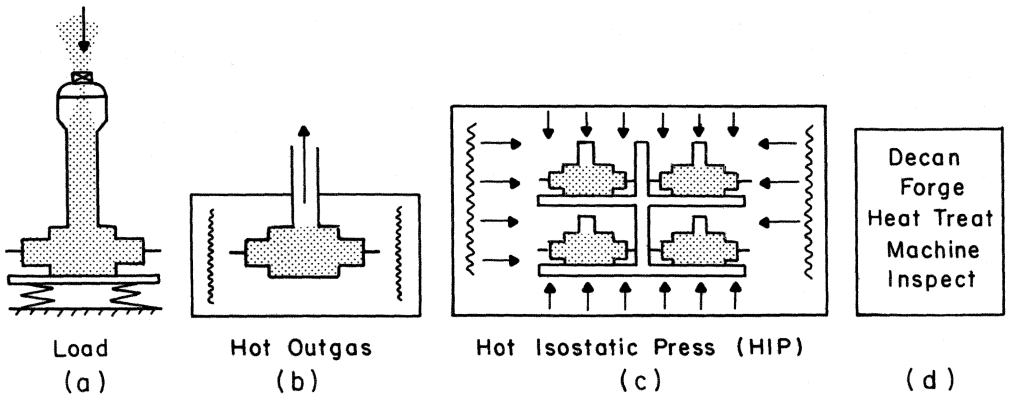

FIGURE 7. The hot isostatic pressing (HIP) process; (a) loading powders in can; (b) hot outgassing; (c) exposure to specified temperature at a specified pressure causing bonding; (d) subsequent processing steps. (From (19), p. 38).

for separations beyond 1 to 2 nm. Nearest neighbor distances are not precisely characterized and these separations are often up to 5 pct larger than in the crystallized phase. For some alloys the difference can be as high as 10-15 pct (8). Structure factors obtained from electron diffraction studies (9) show that the characteristic curve for an amorphous metal has a well defined first peak followed by a split second peak suggesting that this state of aggregation is somewhere between that of a liquid and a microcrystalline metal. Similar structure factors have also been obtained for amorphous alloys consisting of a transi-

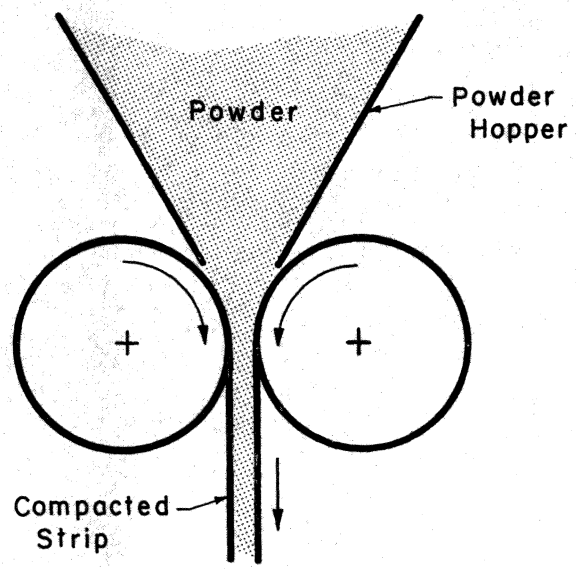

FIGURE 8. Powder rolling; powder is fed through hopper to space between rolls.

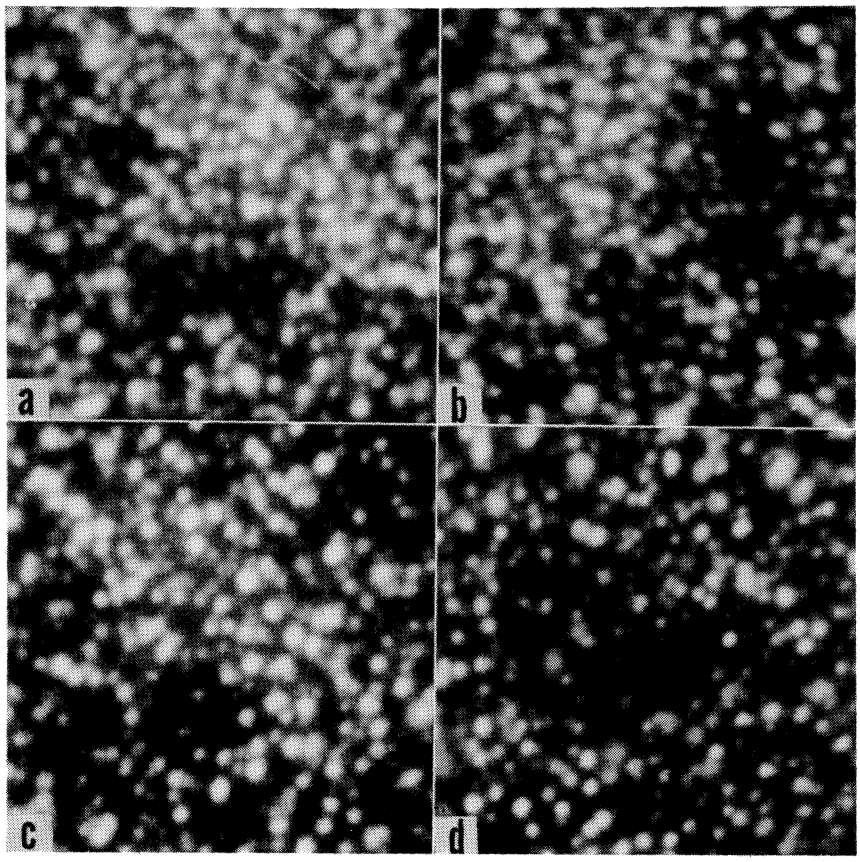

FIGURE 9(a-d). Field-evaporation sequence through amorphous $Fe_{80}B_{20}$ alloy; neon imaging medium at 78K.

tion metal-metalloid composition. Density measurements, on the other hand, indicate that metallic glasses can be as close packed, atomistically, as the FCC and HCP crystalline aggregation.

To date, amorphous alloy compositions have mostly been tailored for a specific need. When high strength, hardness, and ductility are desired, compositions containing Fe and B have been consistently produced. For improved corrosion resistance and reduced stress corrosion, alloys containing Fe, Cr, Ni, P, and C have been quenched into the amorphous state. The state of the art in this domain has reached the point that a very specific need can be answered with the needed composition for the optima in that requirement. A good example in this regard is the Allied Chemical Metglas alloy 2605 SC; it has the best possible soft magnetic properties ever achieved (10).

Although even pure metals have been quenched to the amorphous state, some doubt exists about contamination playing a major role in the stabilizing of the random atomic aggregation. In this regard, Fe, Co, Ni, and Cr are thought to be the best candidates. The general groups that have been successfully quenched into the amorphous form include:

a) Transition metal-metalloid: Ni-P, Pd-Si, Fe-P-C, Ni-Pd-P are examples.
b) Transition metal-rare earth element: Co-Gd, Ni-Dy are some candidates.
c) Noble metal-rare earth element: Co-Gd, Ni-Dy are some candidates.
d) Others: such as Fe-Au, Cu-Zr, Nb-Ni and a whole host of other examples signify the possible groups.

Recent successes in the generation of wear resistant surfaces utilizing laser passes and ion implantation owe their improved properties to the generation of thin amorphous layers on these surfaces by the exposures to laser and high dose ion implantations. In the former case the quick-quench from the molten state is utilized while the latter procedure capitalizes on the fact that the implanted specie stabilizes the disorder generated by the high energy bombardment of the surface.

The crystallization behavior of most amorphous alloys are seen to be a function of (11):

a) temperature of crystallization,
b) time at temperature, and
c) heating rate.

These three parameters are seen to be instrumental in the ease of retention of the non-crystalline structure as well as the sequence of metastable phases achieved previous to the attainment of the final equilibrium phase mixtures.

In many cases crystallization occurs progressively, rather than directly, through a sequence of non-equilibrium phases to a fully stable equilibrium phase or phases (12,13). Depending on the constituent elements, crystallization can occur by one of three possible reactions (14):

a) Polymorphous crystallization; is the crystallization of the amorphous alloy without any change in concentration into a supersaturated, metastable or stable crystalline alloy. The supersaturated alloy will go through subsequent precipitation reactions and the metastable alloy will undergo phase transformations into the stable equilibrium phases. This type of reaction is limited to concentration ranges near the pure elements or the compounds.

b) Primary crystallization; is the recrystallization of one of the stable phases having a different composition than that of the original amorphous matrix. The remaining amorphous matrix can transform later, at the same or higher temperature, by one of the three mechanisms discussed here. The dispersed primary crystalline phase may act as preferred nucleation sites for the subsequent crystallization of the amorphous matrix.

c) Eutectic crystallization; is the simultaneous crystallization of two crystalline phases by a discontinuous reaction. This reaction has the largest driving force and can occur throughout the entire concentration range between the two stable phases. Although there is no concentration difference across the reaction front, the two phases must separate in the reaction front. Therefore, this reaction takes more time than the one where no phase separation occurs, i.e., the polymorphous crystallization.

Many properties of metallic glasses, such as density, heat capacity, and compressibility are very similar to their crystalline counterparts, as indicated earlier. Differences are seen to arise in those properties that measure the response of the alloy to a directed force. The crystalline structure which inherently induces anisotropy in response to magnetic, electrical or mechanical forces is absent in metallic glasses, thus leading to a greater degree of isotropy.

In response to a mechanical force, i.e. tension, a metallic glass reacts much differently than a crystalline metal or a silica-based glass. A crystalline metal yields by the movement of defects along specifically defined slip planes which leads, generally, to strain hardening and an increase in resistance to further deformation. In a Metglas alloy, however, there are no slip systems and thus no strain hardening. When an amorphous alloy yields it does so at an angle of about 45 degrees to the applied stress (15). Figure 10 illustrates shear bands in an amorphous sheet deformed by bending.

Shock induced deformation of amorphous alloys $Fe_{80}B_{20}$ and $Fe_{38}Ni_{40}Mo_4B_{18}$ (15 and 25 GPa for 2 μs duration) is seen to yield no microhardness or discernible structural alterations. Simultaneously shocked crystalline

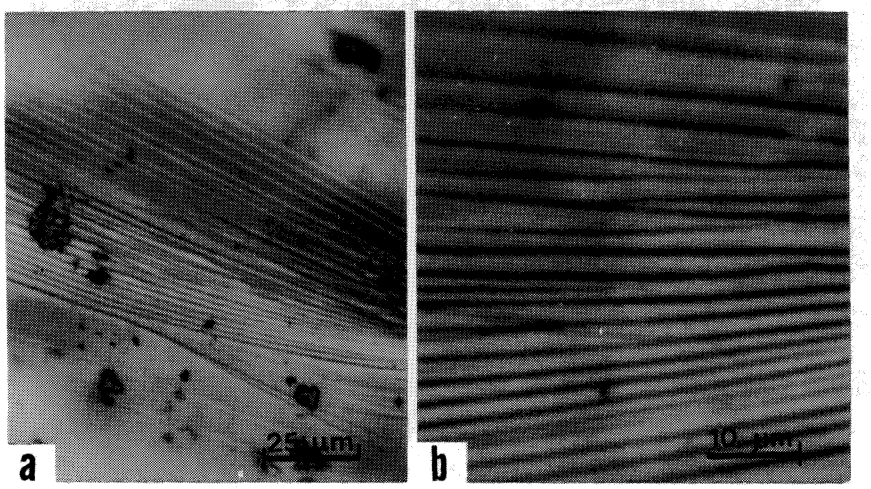

FIGURE 10 (a&b). Shear bands amorphous alloy 2605 SC, deformed by bending.

metals (Mo & W), however, exhibit microhardness increases with increases in peak pressures and the induced defect structure is seen to consist of mono and aggregate vacancies as well as an increased dislocation loop density (16). It is believed that peak pressures in excess of 90 GPa are required to result in a heating effect that would induce crystallinity and thus a structural change in amorphous alloys. Figure 11 (a-b) shows field-ion micrographs of shock loaded amorphous sheets.

Exposure to a Q-switched ruby laser (25 ns pulse width at half max.) beam of 22 and 35 J/cm^2 fluence is seen to produce vaporization, melting, and spallation in W and Mo samples which can be approximated to correspond to the residual effects of several hundred kbar peak pressure shock waves. Two pulses at the higher fluence (35 J/cm^2) irradiation are seen to induce phase changes in the amorphous $Fe_{80}B_{20}$ alloy. The point of impingement exhibits the equilibrium phase mixture of α(Fe) + Fe_2B while the surrounding zones are seen to consist of α(Fe) + Fe_3B + Fe_2B, α(Fe) + Fe_3B and α(Fe) in an amorphous matrix with gradual increase of distance from the point of impingement (17). Some example micrographs are shown in Figure 12(a-b).

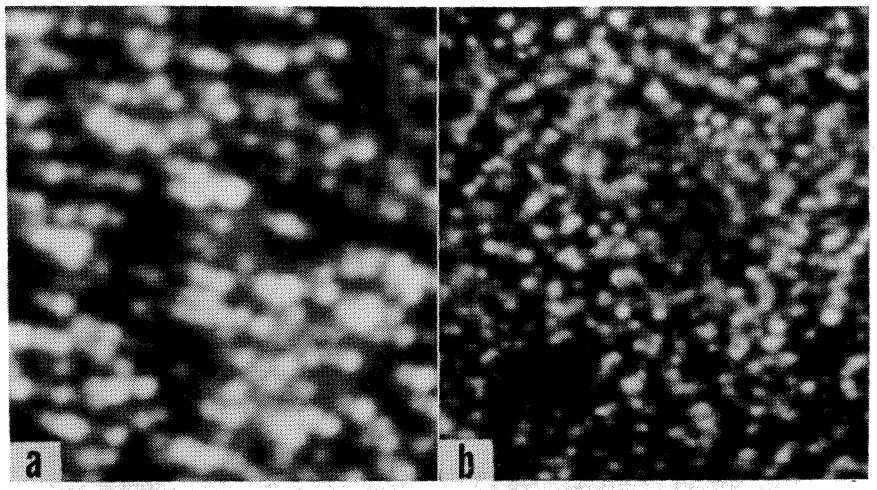

FIGURE 11(a&b). Amorphous alloy $Fe_{80}B_{20}$ shock loaded to 150(a) and 250(b) kbars.

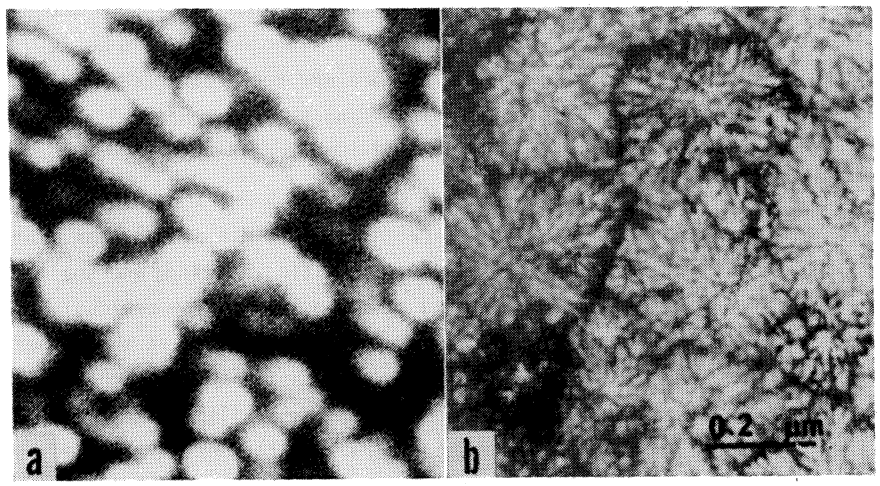

FIGURE 12(a&b). Laser induced damage to amorphous alloy $Fe_{80}B_{20}$. Crystallization induced with 35 J/cm^2 deposition as seen in an FIM(a) and TEM(b).

Four amorphous alloys ($Ni_{50}Nb_{50}$, $Fe_{80}B_{20}$, $Ti_{30}Cu_{70}$ and $Ti_{60}Ni_{30}Si_{10}$) exposed to high energy proton irradiation (800 MeV) exhibit no discernible structural alteration while Mo and W samples, simultaneously irradiated, show an increased vacancy and vacancy-cluster densities as well as void formation (18).

Finally, amorphous alloys are considered resistant to corrosion and experiments indicate that, especially compositions containing Cr and P, excell in this regard. The explanation given for the improved corrosion properties is the formation of a non-crystalline passive film on these alloys that consists of a chemically homogenous, single (random) phase.

Previous to the utilization of the superior magnetic, strength, and corrosion resistance properties of amorphous alloys, an understanding of the atomic aggregation is necessary. Although several theories attempt to model the atomic aggregation, none are based on direct atomic analyses, and only a very few of the superior properties of these alloys are, therefore, explained.

IV. OXIDE DISPERSION STRENGTHENING AND MECHANICAL ALLOYING

In dispersion-strengthened materials, the second phase (strengthening phase) is not introduced by means of the phase diagram (precipitation or spinodal decomposition). Rather, it is added in the fabrication process. High melting-point oxides are preferred, and superalloys show much enhanced high-temperature creep resistance when strengthened by dispersions. These dispersions form an incoherent boundary with the matrix; at high temperatures these boundaries attract dislocations, since the poor interfacial bonding makes the site act as a hole. A dislocation segment is shortened by intersecting a dispersoid. Two different processing schemes are used to introduce these powders into the matrix; a wet and dry method.

T-D Nickel is a nickel alloy with a dispersion of 2 pct. of thorium oxide (19). It is produced by precipitating nickel hydroxide from a nickel salt solution. This solution has thoria in colloidal suspension. The precipitate is dried and then reduced in hydrogen. The powder is then processed by HIP or hot extrusion.

The latest ODS superalloys use Y_2O_3 instead of thoria, because of the radioactivity of the latter. Mechanical alloying is the technique used to bond the metal powders to the ceramic powders. Figure 13 shows the processing sequence used. The powder mixture is introduced in a ball mill driven by a rotary impeller. The powders are crushed between the spheres; this process involves deformation, fracture, rewelding of the fragments and incorporation of the yttria particles into the superalloy powders. Figure 14 shows the process of formation of these composite particles from the deformation between two steel balls. The deformation creates gaps on the surface layer, exposing atomically clean metal.

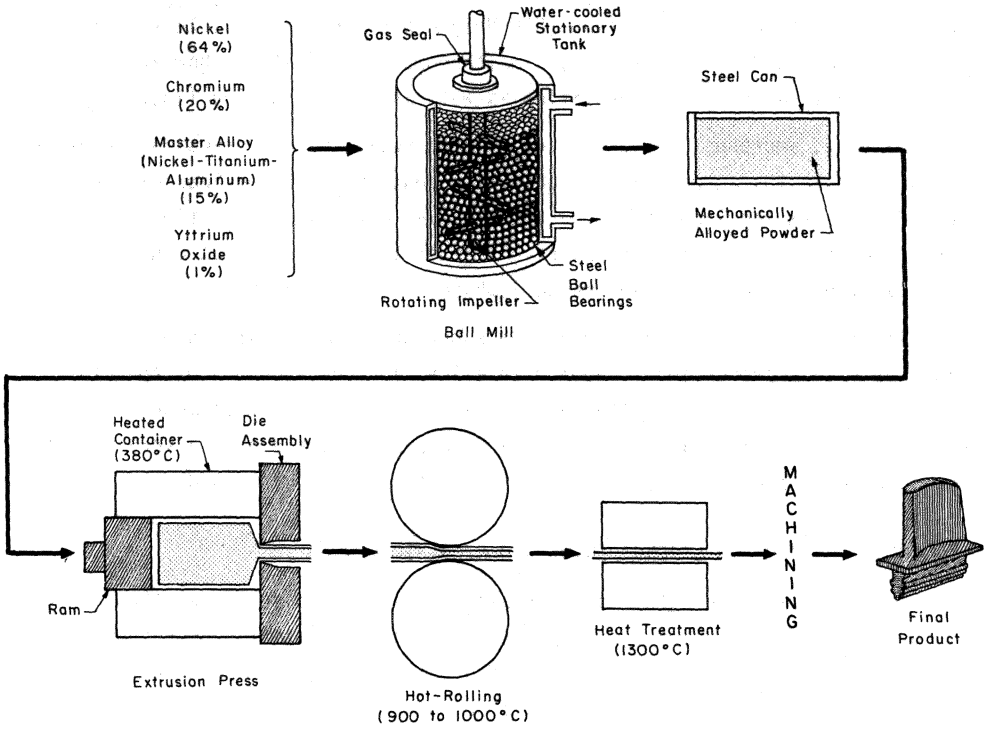

FIGURE 13. Processing sequence in the production of mechanically alloyed turbine blade (Adapted from J.S. Benjamin, Sci. Am., 234, No. 5 (1976) 40, Figures on pages 42 and 43).

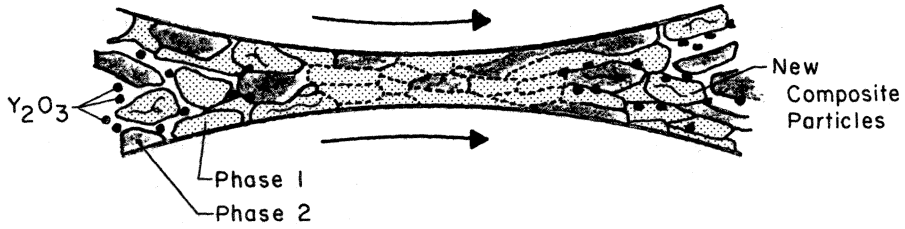

FIGURE 14. Formation of mechanically-alloyed powder from three different constituents by compression and shear between two spheres; notice composite particles (containing phases 1 and 2 and Y_2O_3 particles) being formed on right-hand side (Adapted from J.S. Benjamin, Sci. Am., 234, No. 5 (1976) 40, Figures on pages 42 and 43).

These clean surfaces weld together, under pressure. After the mechanically alloyed powder is produced, it is usually canned, hot extruded, hot rolled, and heat treated (Fig. 13).

Figure 15 shows the 1000-hour rupture strength of the ODS superalloy MA 6000E (20). At higher temperatures the behavior of this alloy is dramatically better than that of conventionally processed IN-792. At 1100°C, when the 1000 hour rupture strength of IN-792 and directionally solidified MarM-200 (with hafnium additions) drops to nearly zero, the strength of the ODS alloy MA 6000E is 150 MPa. The low temperature strength of the mechanically alloyed material is as high as that of conventionally processed material, while in TD Nickel (also dispersion strengthened) the room temperature strength is very low.

V. OTHER PROCESSING INNOVATIONS

Numerous innovative processing techniques have been developed or are being developed. Many of them are covered in other sections in this chapter and in other chapters. A few special techniques are described here.

Superplastic forming is a technique taking advantage of the outstanding ductility exhibited by some alloys at specific temperatures and strain rates. The *sine qua non* condition for superplasticity seems to be a small grain size. Defor-

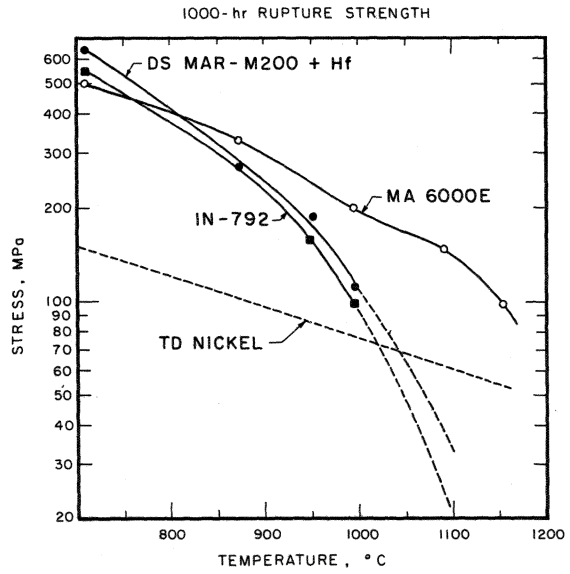

FIGURE 15. Rupture stress (at 1000 hours) as a function of temperature for mechanically alloyed MA 6000 E, thoria dispersed nickel, and conventional superalloys DS MAR-M 200 (Hf) and IN-792 (Adapted from (20), p. 10).

mation takes place by grain boundary sliding, primarily, and the grain shape does not undergo plastic changes. For example, the aluminum - 5 pct calcium - 5 pct zinc alloy with a 1-2 μm grain size can exhibit an elongation of 7200 pct at 450°C. Superplastic response has been obtained in aluminum alloys (aluminum-copper, aluminum-calcium, aluminum-magnesium-zinc), titanium alloys, zirconium alloys, zinc alloys, superalloys, and high-carbon iron alloys (21). The large plasticity has made these alloys amenable to processing techniques usually applied to plastics. Hence, superplastic zinc alloys are successfully vacuum molded. However, a positive pressure allows a better control of the strain rate. Figure 16 shows a superplastic forming process used in the fabrication of Ti-6Al-4V panels. Three layers of titanium sheet are placed on top of each other, with spacers. Pressure and heat are applied, promoting diffusion bonding (DB) of the regions without spacers. Gas pressure is then applied by means of the tube shown, causing the expansion of the panel.

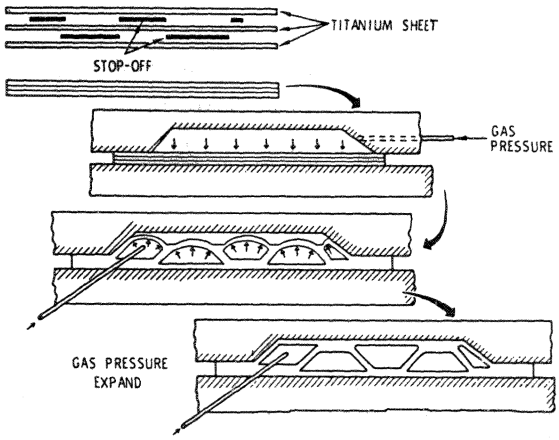

FIGURE 16. Superplastic forming (SPF/DB process) for sheet parts (From (21), p. 380, Fig. 44).

Innovations in the processing of steel have also led to great improvements. Great strides are being made, besides the development of new alloys (such as microalloyed and dual-phase steels) in the careful processing of steel. Clean steel technology has led to substantial improvements in the mechanical properties, including fracture toughness, ductility, and fatigue resistance. Commercial steels have substantial amounts of impurities, and oxygen and sulfur are two important ones. Oxides and sulfides have well-known deletereous effects on the strength. Phosphorus and hydrogen are two embrittling elements. What is commonly referred to as "clean steel technology" is a whole range of treatments applied with the objective of reducing the impurities of steel (22, 23). The most common processes are:

Vacuum induction melting (VIM)
Vacuum arc remelting (VAR)
Vacuum degassing (VD)
Argon oxygen decarburization (AOD)
Electron beam refining (EBM)
Electron slag remelting (ESR)

Plasma has been called the fourth state of matter. At temperatures above 2000 K gas molecules dissociate themselves into individual atoms. In the temperature range 2000 - 3000 K a considerable fraction of the gas atoms lose electrons and become ionized. The electrical conductivity of plasma is of the order of that of melting salt (or slag): 10-100 $\Omega^{-1}cm^{-1}$. In general, there are three methods for obtaining plasma, schematically illustrated in Figure 17. In Figure 17(a) the plasma is generated between electrodes; the plate is negatively charged and the rod positively charged. Figure 17(b) shows the plasma torch; the gas flows through the electrode. Figure 17(c) shows the induction-coupled torch, which generates the so-called induction plasma or electrodeless plasma. Figure 18 shows the relationship between temperature and density in the plasma state. The temperature is expressed in eV (1eV = 11,605 K). The plasmas of interest for metallurgists are in the range of 10-250 eV. This corresponds to the energy range of a glow discharge. The unique characteristics of plasmas are being utilized materials processing: electric arc furnaces, plasma arc welding, plasma arc spraying, vacuum arc melting, plasma arc melting, plasma reactors in extractive metallurgy, ceramic and glass applications of plasma technology are technologically important fields (24-26).

The utilization of plasma in the production of steel will be briefly described here (24). It provides an alternative to the traditional routes. The principal advantage of plasma is that the thermal energy is separated from the

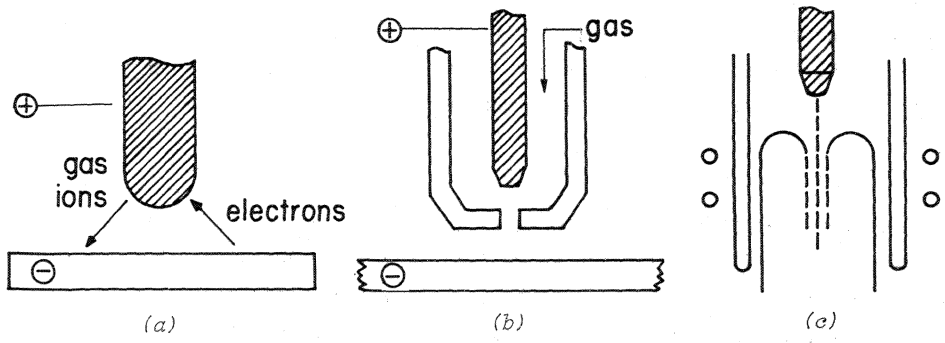

FIGURE 17. The three principal methods for generating thermal plasmas; (a) plasmas between electrodes; (b) plasmas through electrodes; (c) the induction-coupled torch. (From (24), p. 58, Fig. 3).

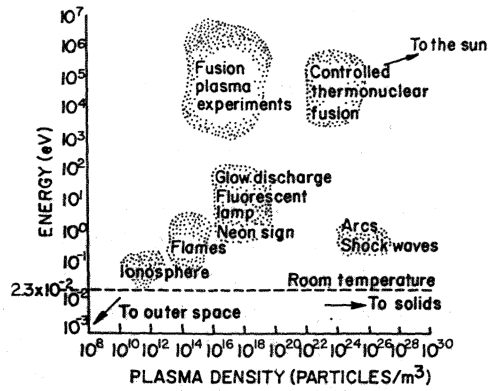

FIGURE 18. Energy-density diagram of the plasma state (From (24), p. 58, Fig. 4).

reduction reaction. In the blast furnace and in direct reduction, the reduction reaction gases and the heat come from the same source. The application of plasma provides one additional degree of freedom in processing: the plasma is the source of energy, while the reducing agents are independently added to the reaction chamber. This added degree of freedom and the high energy density attainable in plasma lead to excellent pollution control and to smaller process vessels, respectively. The Plasmared and Plasmamelt processes developed in Sweden represent a significant break from traditional BOF and DRI practices. Figure 19 shows the flow diagram for the Plasmamelt process. It consists of two stages, in separate units. First, the ore is prereduced in two fluidized bed chambers resulting in 50-60 pct. reduction. Secondly, the pre-reduced ore is mixed with limestone, pulverized coal, and plasma-heated gases are injected into a chamber filled with coke for final reduction. The plasma torches reach temperatures up to 5,300 K. The function of the coke bed is not to act as a reducing agent; it provides a permeable reaction zone in the shaft and protects the refractory lining of the furnace. The Plasmamelt process uses 16 pct. less energy (electrical + coke + coal) than the blast furnace.

VI. MODIFICATIONS IN SURFACE PROPERTIES

Incorporating elements into surfaces and/or the addition of surface layers for wear and corrosion resistance as well as decorative appeal has been practiced for a long time. In this regard, some of the surface oxides generated (such as Cr_2O_3, ZnO etc.) have since been utilized in the generation of photothermal solar-selective surfaces, at much smaller coating depths, in recent years.

Surface mechanical property improvements of steels have relied on either deposition processes (plating, anodic oxidation) or the generation of a surface

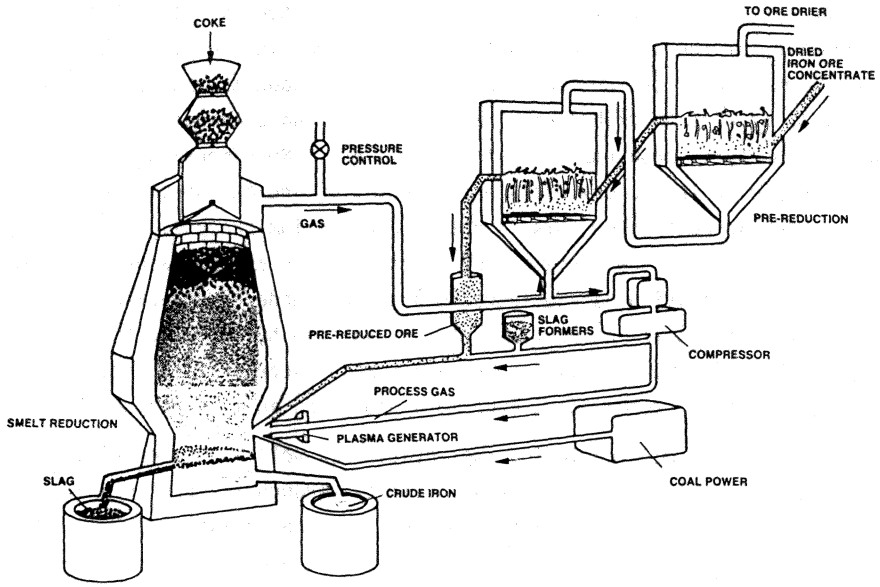

FIGURE 19. The Plasmamelt process developed by SKF (From (25), p. 30).

"case region" by thermally-based techniques such as nitriding, carburizing, boronizing, induction hardening, flame hardening, and, more recently, laser hardening. These procedures are widely used in practice and, for most applications, seem to be the most economical methods of surface property improvements. However, new techniques have been or are being developed, and will be highlighted in Sections VI (A) and (B).

A. Ion Implantation

With the incorporation of "plasma technology" into the surface alteration domain, many new techniques have evolved that span from ion-plating to ion-implantation of gaseous or metallic species. The power requirements increase, by an order of magnitude, within this span and thus the expense of the surface modification increases several-fold making it practical for special applications only.

Bulk property alterations which inherently occur are the main objection to the thermally-based techniques of surface modification. Another requirement that limits their application for today's needs includes the fact that equilibrium reactions are involved which limit the inclusion of ionic species to surfaces, that would induce the highest hardness and lowest friction parameters. Formation of undesirable intermetallic inclusions is also a consideration to be dealt with that can lead to a weak bonding at the case/core interfaces.

With ion-implantation a specie is injected into a surface at temperatures where bulk properties are unaltered. Thus, what is created is not a coating but the continuation of the same specie with slight changes in the stoichiometry. This arrangement affords better mechanical attachment, good thermal contact for the dissipation of heat in tribological applications, and a homogeneous coating that avoids porosity problems of coated overlayers. No dimensional change, in the macroscopic scale, occurs with ion implantation and any specie deemed needed can be implanted. Since this is not an equilibrium process, solubility considerations as well as the formation of brittle phases are not a problem (27). If the concomitant radiation damage introduced can be rendered non-catastrophic, amorphous layers with their inherent advantages can also be produced through ion-implantation (28). However, laser hardening, also incorporating simultaneous carbon powder injection, seems to be much more promising in this regard (29).

The mechanism of hardening in ion-implantation as well as in thermally based techniques is the reduction in dislocation mobility through the presence of the specie incorporated into these surfaces. The role of the radiation damage introduced in the former case is not quite clear yet. Much progress is being done in terms of understanding of ion-implantation, but not much effort is involved in the optimization of the conventional methods that utilize much lower current densities and power requirements; although these methods are still inexpensive enough to be practical and are certainly within the realm of answering the needs of today's technology. A mathematical modeling of all process variables, to optimize a surface hardness at a given case depth, would not only lead to the development of economic procedures but also lead to the understanding of the property alteration mechanisms of those and other techniques. The surfaces hardened with ion-nitriding procedures, for example, seem to be consistent in homogeneity, thickness, as well as microhardness properties and are seen to have much improved wear, friction and corrosion properties. The bulk microstructure is seen to be unaltered through the ion nitriding duration and no discernible dimensional change is seen to be introduced in these steel samples (30,31). An example of the structural features produced by ion-nitriding, in the case hardened region, is shown in Figure 20.

B. Laser and electron-beam glazing (32,33)

Laser and electron beams can deposit high energy fluxes to the surface of metals. This ability has been explored technologically and feasible processes are emerging. A number of modifications of surface properties can be achieved through:

a) The surface can be melted and rapidly resolidified;
b) Alloying elements can be added to the surface in conjunction with the beam;

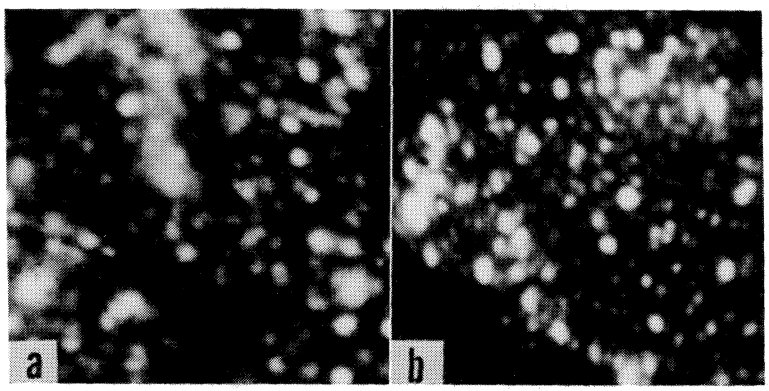

FIGURE 20(a&b). Ion nitriding features of AISI 6150 steel; (a) the tempered structure exhibiting carbides, and (b) fine metal-nitrides formed following ion-nitriding.

c) Pulsed high-power laser can generate shock waves in the sub-surface layers with a resultant strengthening;

d) Lasers can be used to anneal the surface.

Figure 21 shows the results obtained by Draper (33) on laser surface-alloying AISI 1018 steel. The case-hardened depth is approximately 0.1 mm thick. The concentrations of carbon, chromium, and manganese are substantially higher in the surface region. The pre-irradiated films were sprayed on and consisted of particles of 10-50 μm diameters suspended in alcohol.

Laser glazing is schematically shown in Figure 22. A high-power continuous CO_2 laser beam is focused on the metal surface (spot diameter ~0.5mm). This high-power laser promotes the melting of the surface, in spite of the high reflectivity of metals at the wavelength of CO_2 lasers (10.6 μm). An inert gas is applied to the region, in order to suppress plasma generation and oxidation of the melt pool formed. The metal parts are placed on a rotating tray. The rate of cooling of the molten metal is determined mainly by the thickness of the layer and by the thermal conductivity of the metal. Rates of cooling that can be achieved are in

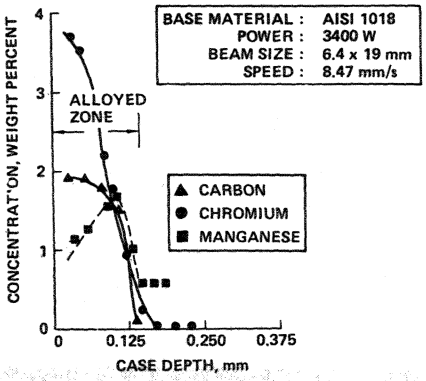

FIGURE 21. Cross-section of laser surface-alloyed 1018 steel. Laser processing parameters and concentration profiles given in Figure (From (33), p. 28, Fig. 5).

the range 10^6-$10^8 K^{-1}$; this is well in the realm of rapidly-solidified materials. Hence, the range of microstructures observed includes microdendrites, ultra-fine eutectics, extended solid solutions, metastable phases, and amorphous layers. This process has shown promising improvements in corrosion, erosion, and wear properties. Surface hardening of M2 tool steel has led to improvements in performance.

The application of laser beam in conjunction with surface alloying also presents bright prospects. The alloying elements can be added to the surface either before or during the laser-glazing process. The continuous delivery of material to the laser-molten zone is called layer-glazing or incremental solidification. Layer-glazing can either be applied as one layer, for the improvement of surface properties, or as a succession of layers, building up a bulk rapidly solidified structure. Figure 23 shows examples of the utilization of layer glazing for the

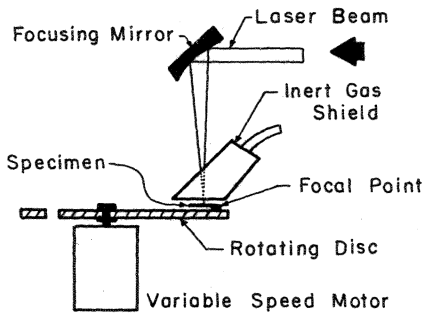

FIGURE 22. Schematic illustration of laser glazing apparatus; inert gas shield is required in "glazing" zone (From (32), p. 322, Fig. 2).

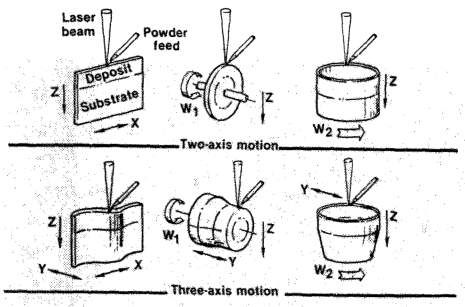

FIGURE 23. Examples of layer glaze processing for near-net shape. The layers of material are successively deposited on the substrate, building up the part. (From (32), p. 331, Fig. 23).

production of bulk components. Depending on the shape of the product, two-axis or three-axis motion is employed. This requires the use of a computer-controlled work station. The utilization of layer glazing for valve seats, turbine blade tips, bearing surfaces, and gas-path seals is being explored.

Electron-beam glazing is similar to laser beam glazing; it presents the advantage that the beam can be scanned over the surface of the specimen by means of magnetic deflection coils.

VII. MARTENSITIC TRANSFORMATIONS

Professor M. Cohen and Dr. G.B. Olson present, in Chapter 2 , fundamentals and advances in the understanding of martensitic transformations; in Chapter 3 Professor Thomas describes the structure, properties, and present and potential applications of martensitic transformations. Martensitic transformations continue at the frontier of metallurgy, and enhanced understanding has led to new applications. Figure 24 shows the classic lenticular shape of martensite. The lens shows a central line, called mid-rib. Other morphologies are also observed in other systems: needle-shaped, butterfly, lath, segmented plates, and thin plates. The discussion in this section will restrict itself to thermoelastic martensite, not treated in the other chapters. The shape-memory effect (SME) is the unique property that some alloys possess according to which, after being deformed at one temperature, they recover the original shape upon being heated to a second temperature. The built-in memory is produced by the martensitic transformation. The effect was first discussed by the Russian metallurgist Kurdjumov. In 1951, Chang and Read (34) reported it for an In-Tl alloy. However, wide exposure of the properties came only after the development of the nickel-titanium alloy (NiTINOL) by the Naval Ordance Laboratory in 1968 (35). Since then, the research activity in this field has been intense, and the following β-phase SME alloys have been investigated: AgCd, AgZn, AuCd, CuAl, CuZn, FeBe,

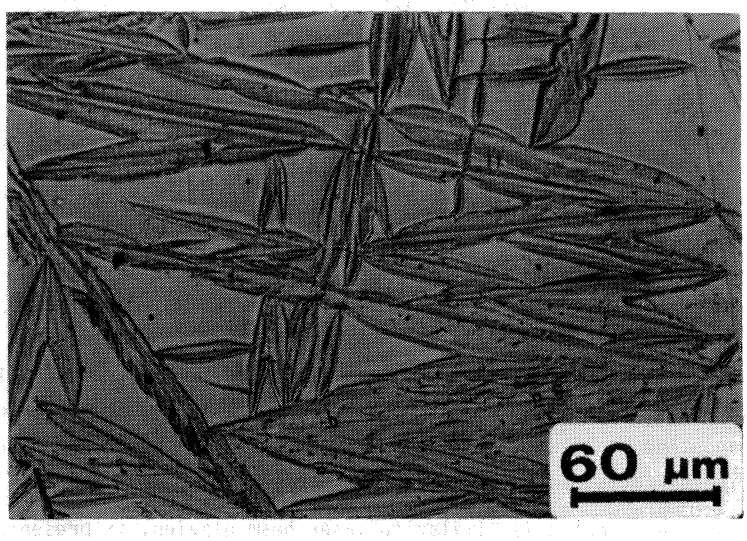

(a)

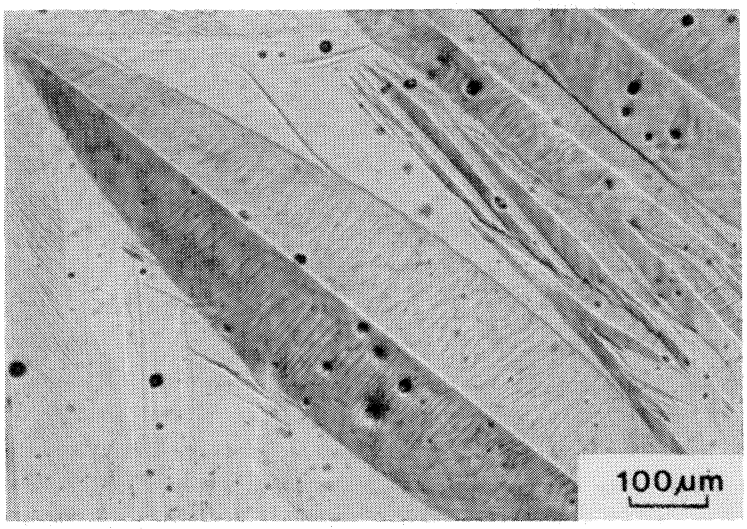

(b)

FIGURE 24. Optical micrographs of martensite;(a) lenticular martensite in Fe-32 pct Ni-0.035 pct alloy (Courtesy of N.N. Thadhani, California Institute of Technology).
(b) Thermoelastic martensite in Cu-Al-Ni alloy (Courtesy of R.J. Salzbrenner, Sandia National Laboratories).

FePt, NbTi, NiAl, and ternary alloys. The Nitinol family of alloys has found wide technological applications, and adjustments in the composition can be made to produce M_s temperatures between -273 and 100°C. This is an extremely helpful feature, and alloys are tailored for specific applications. In the majority of SME alloys the high-temperature phase is a disordered phase (body-centered cubic), while the martensitic phase is an ordered BCC structure with a superlattice or orthorhombic structure. Two separate mechanical effects characterize the response of SME alloys: pseudoelasticity and strain memory effect. They will be described in connection with tensile tests.

Pseudoelasticity is the result of stress-induced martensitic transformation in a tensile test which reverts back to the parent phase upon unloading. The individual martensite plates do not grow explosively, as in the ferrous martensites, and little irreversible damage is done to the lattice. The shear strain of one plate is accommodated by neighboring plates. The complex motion of the interfaces between the martensite plates along the various variants and within the same martensite plate, takes place by the displacement of the interfaces between the different twins.

When the deformation is irreversible, the name "strain memory effect" is used. Additional heating is required to revert the martensite, since the deformation temperature is below A_s. Upon heating, the original dimensions will be regained, as the martensite interfaces move back to retransform the lattice. The sequences in which the plates form and in which they disappear are inverted. The first plate to form is the last to disappear.

The strain-memory effect is also obtained when deformation is imparted at temperatures below M_s. This is actually the procedure used in most technological applications. In this case, the structure consists of thermally induced martensite; it is present in such a way that all variants occur. When the external stress is applied, the variants that have shear strains aligned with the applied shear strain tend to grow and the unfavorably oriented variants shrink. Figure 25 shows schematically how this takes place. Only two variants are shown, for simplicity. The variant that favors the applied tensile strain grows at the expense of the unfavorably oriented one. Hence, all unfavorable variants disappear and the favorable variant takes over the structure. On heating, the structure reverts back to the original one, composed of equal distribution of the two variants, giving the strain recovery.

The shape-memory effect can be described from the point of view of technological applications as a "solution looking for a problem" (36). It has found some unique uses. One is as a tight coupling for pneumatic and hydraulic lines. The F-14 jet fighter tube couplings are made of Nitinol that is fabricated at

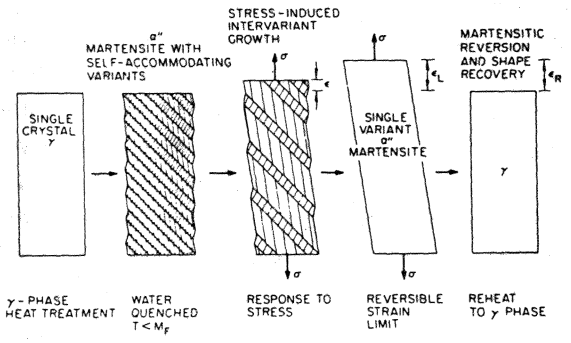

FIGURE 25. Sequence showing how growth of one martensite variant and decrease of others results in strain ε_L (Courtesy of R. Vandermeer, U. of Tennessee).

temperature with a diameter 4 pct less than that of the tubes that will be joined. Then, the couplings are cooled below M_S (- 120°C) and expanded mechanically until their diameter is 4 pct larger than those of the tubes. They are held at this temperature until they are placed over the tube ends. Allowed to warm, they will shrink to the initial diameter; impeded by the tube, they will provide a tight fit. Electrical connectors that are opened and closed by temperature changes are another application. Orthopedic and orthodonic aids have also been tested, and Nitinol seems to react well in the body fluid environment. The pen-drive mechanism in recorders is a very successful application of the SME; over 600,000 of these new drives are now in service. Another application that has received a lot of attention is the utilization of the SME in the direct conversion of heat to mechanical work. The advantage is that such an engine can utilize low-temperature gradient thermal sources (~20°C). However, its efficiency is very low.

VIII. SHOCK-WAVE PROCESSING OF MATERIALS

The utilization of explosives for welding, forming, cladding, strengthening, consolidation, and cutting of metals is well established. Commercialization of explosive welding dates from 1964 (37) and the annual volume of operations (in the Western World) is close to $40 million. Explosive welding allows bonding of metals with widely different melting points and metals that cannot be welded by conventional means. The most simple geometry is illustrated in Figure 26(a). The high-velocity impact of the top plate on the bottom one causes a liquid jet which cleans the surface and allows a metallurgical bond to take place. Figure 26(b) shows the characteristic wave appearance of the bond. While this technology is well developed, there are new concepts being developed. One of them is explosive cladding of amorphous metal ribbons on metal base.

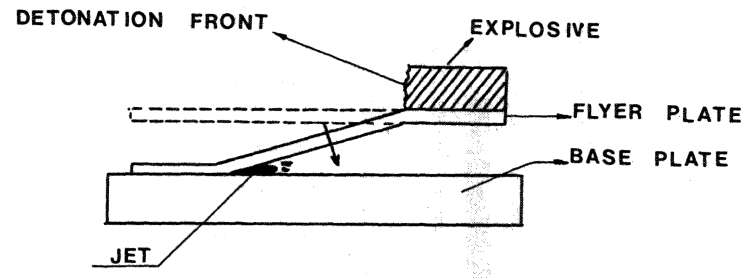

(a)

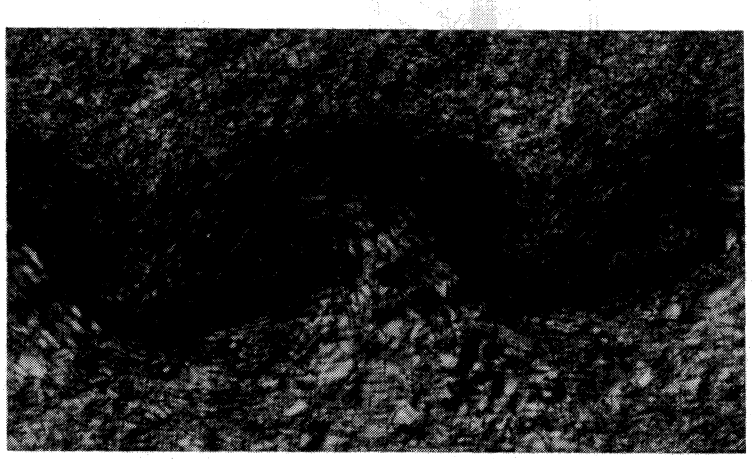

(b)

FIGURE 26(a) Parallel-plate geometry for explosive welding.
(b) Characteristic wavy interface formed by explosive welding.

Dynamic consolidation of rapidly-solidified powders is another area of considerable interest. The unique microstructures generated by rapid solidification can be destroyed by high temperatures. One of the techniques to produce bulk materials from the powders is by utilizing explosive energy. Figure 27 shows a set-up used for explosive consolidation. The metal powder is placed in a metal tube and surrounded by explosives. Detonation,starting at the top, creates a shock wave which, if all experimental parameters are correct, assures good consolidation. Figure 28 shows optical micrographs of rapidly solidified MarM-200 powders (Fig. 28(a)) and amorphous Metglas (Fig. 28(b)) which were consolidated by explosives. The rapidly solidified powders were initially spherical; one can see white pools, which are thought to be due to interparticle melting

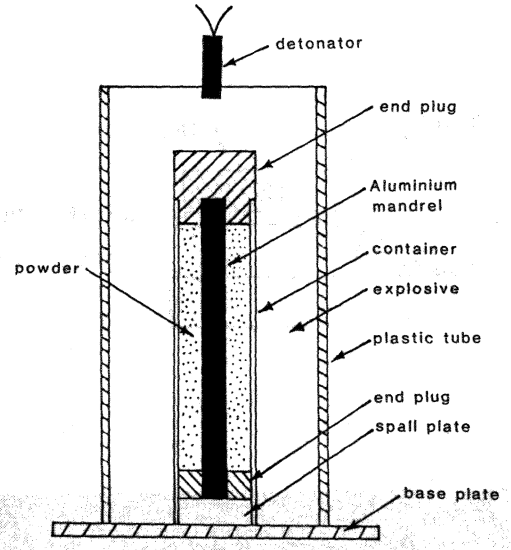

FIGURE 27. Powder compaction set-up. Detonation of explosive (starting at the top) causes implosion of cylinder and high-pressure pulse to travel through powders, compacting and consolidating them.

produced by the quasi-adiabatic deformation and internal impact (particle-to-particle impact). While Cline and Hopper (38) reported in 1977 successful welding and consolidation of metallic glasses, the technological problems are far from solved. Cracking is a major problem in both welding and consolidation, and special fixtures incorporating wave tailoring are being developed at the Center for Explosives Technology Research (New Mexico Tech) to overcome some of the deleterious effects of waves.

Another area of considerable interest is the synthesis of new materials by explosives. The pioneering work of de Carli and Jamieson, published in 1961 (39) reports on the formation of diamond from graphite by the passage of a shock wave through the latter. The patent was issued in 1966 (40) and Dupont at present successfully produces diamond commercially. This polycrystalline diamond is used industrially as an abrasive. Soviet and Japanese effort in this field has exceeded U.S. research (41). A number of different ceramics were synthetized by shock waves; shock-induced polymerization was also demonstrated. One of the shock-synthesized materials of greatest technological importance is cubic and wurtzite-type boron nitride. Recently, Sawaoka, Akashi, and Saito (42,43) produced cutting tools by a combination of shock and static pressures presenting exceptional properties. Boron nitride has three polymorphs: graphite-like (g-BN), wurtzite-type (W-BN-hexagonal), and zinc blende-type (Z-BN-cubic). The W-BN produced by shock compression was subsequently sintered under high pressure, resulting in the formation of bulk specimens. These specimens were tested as cutting tools and showed very low wear rates. Figure 29 shows the wear rate of

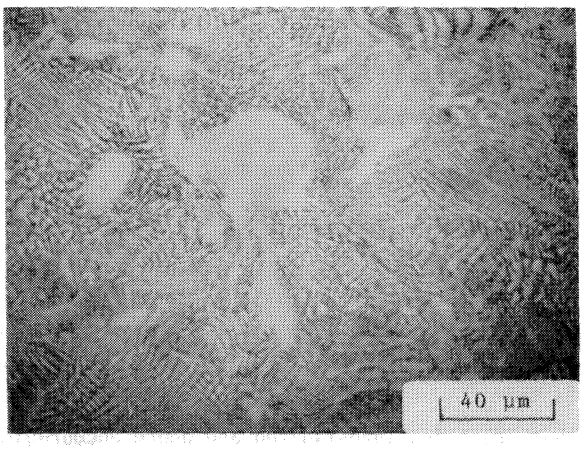

(a)

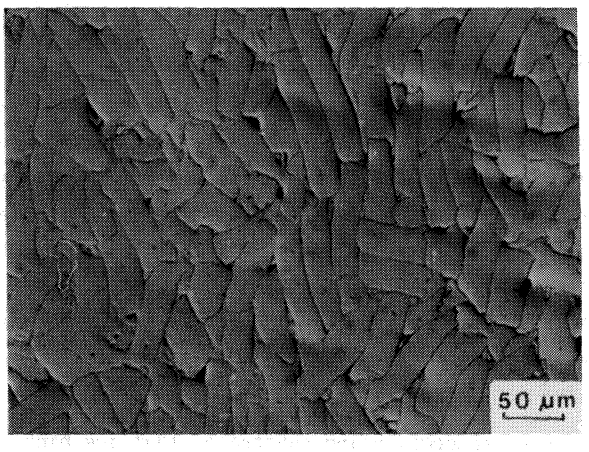

(b)

FIGURE 28. Optical micrographs of explosively-consolidated powders.
(a) rapidly-solidified Mar M-200 powder; melting pockets can be seen as white regions.
(b) metallic glass Metglas 2605.

WURZIN (shock-processed boron nitride) and that of cobalt-bound Z-BN tool. Wurzin's wear rate is less than half that of Z-BN. The cubic boron nitride (Z-BN) is statically synthesized at high pressures. The advantages of the shock-synthesized BN seem to stem from its polycrystallinity, making cleavage fracture during machining more difficult.

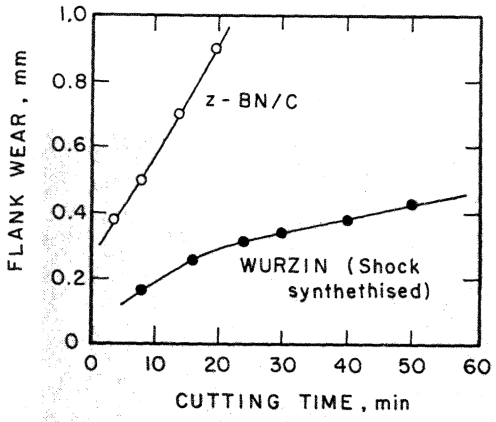

FIGURE 29. Wear rate of tool bits made of shock-synthesized Wurzin produced by Sawaoka and coworkers and Z-boron nitride on tungsten carbide base (From (43), p. 546, Fig. 7)

Other areas that are being investigated and where encouraging results are being obtained is the shock-activation of catalysts and shock-enhanced sinterability of powders (44).

IX. SOLAR-PHOTOTHERMAL APPLICATIONS

Selective (photothermal) solar surfaces may be categorized as low temperature (<250°C) systems used in the flat plate arrangement and high temperature (~300-500°C) coatings produced for focussing collectors with moderately high concentration factors. The features producing selectivity in these coatings can be categorized into intrinsic selectivity of the material, tandem stacks of semiconductors deposited upon reflectors, interference stacks of alternating dielectrics and metals, wave-front discriminating surface roughness, dispersion of metal particles in a metal or dielectric matrix, quantum size effects and oriented overgrowths (45).

Absorber reflector tandems, using substrates that are highly reflecting in the infrared range and covered with a thin but strongly absorbing coating have been thoroughly investigated at low wavelengths. These arrangements combine the solar absorptance of the black deposit with the thermal emittance of the metallic substrate. Of such coatings, black copper (46), which attains part of its selectivity from the intrinsic band-gap of the semiconductor oxide, is a typical example. Structural features of a black zinc overlayer (ZnO) are shown in Figures 30(a) & (b). Black nickel (47) and black chrome (48) are other examples of coatings operating on this principle. Micrographs exhibiting structural features of the black chrome overlayer are shown in Figure 30(c) & (d).

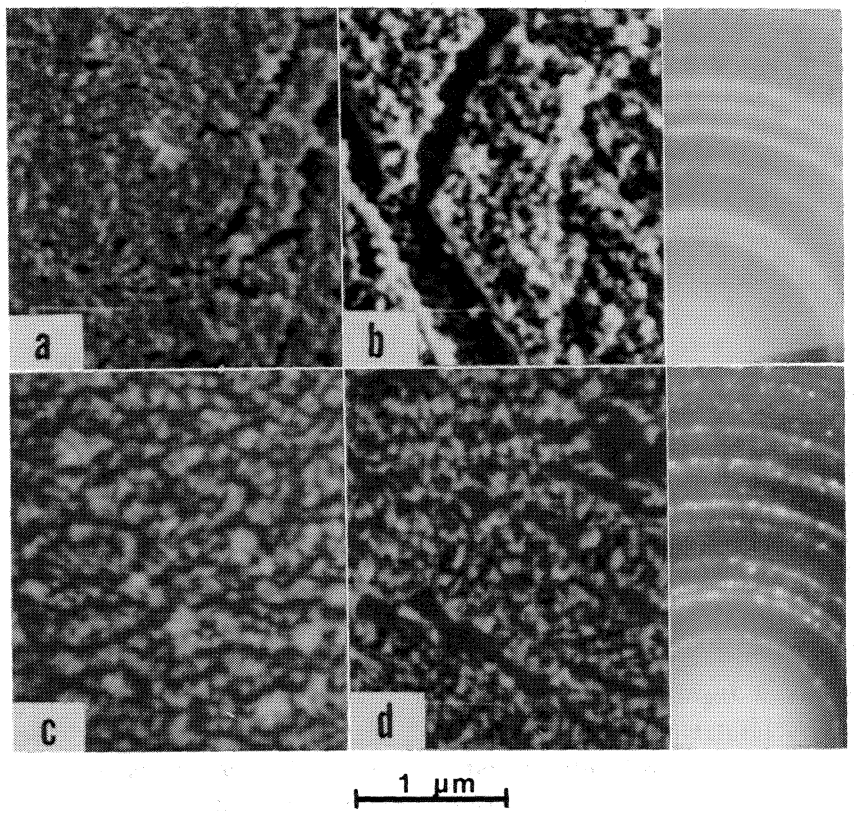

FIGURE 30 a) and b) SEM micrographs of as-plated and heat-treated black zinc coatings. The RED pattern corresponding to the heat-treated surface shows the film to be composed of microcrystalline ZnO. c) and d) SEM micrographs of black chrome, before and after heat-treatment. The RED pattern of the degraded surface shows a microcrystalline Cr_2O_3 pattern. All SEM micrographs are taken at 20000X.

Multilayer interference stacks usually consist of thin dielectric layers separated by semi-transparent films. Excellent high temperature coatings have been produced using this principle (such as Al_2O_3-Mo-Al_2O_3 which maintains selectivity up to above 800°C) (49). However, such films are relatively expensive and difficult to prepare. Similarly, wavefront discriminating selective surfaces have been found to provide good quality semiconductor coatings through the introduction of geometric structural features (pits, dendrites, and cavities) which are too small to affect the thermal infrared radiation, reflected by the substrate, but produce absorption at shorter wavelengths (50).

It is only recently that these efforts (such as wavefront discrimination or absorber-reflector tandem arrangements) have been seen to contribute to produce spectrally selective surfaces. It is thus natural to expect that the selective nature of most of the above mentioned coatings can be delineated through fundamental optical relationships using effective medium theories, and thus depends on the complex refractive indices of the components in the system. In this vein, effective medium theories have provided the necessary correlation between the observed optical properties of selective coatings and the theoretical models that describe the coatings (51). Actual experimental verification, based on experimental data on coatings in the as-deposited state as well as following thermal degration, need to be done to further the understanding initiated with the optimized deposition of these surfaces (46,48,52).

X. INNOVATIONS IN POLYMERS

The applications of polymeric materials to date have capitalized on the ability to mold with ease these low-density materials of controlled mechanical properties that also possess chemical inertness and durability. Progress of polymer technology, though, has been hampered by the complexity of the various problems associated with the synthesis, purification and characterization of their structural features. They are inherently more complex than their inorganic counterparts and this is especially true in the case of their electronic characteristics.

Because of the well separated molecular make-up polymers have, they are electrically insulating or semiconducting at most. Only in the extreme case of graphite, where the molecule consists of a whole sheet of carbon atoms, is the conductivity, parallel to the layers, similar to that of a metal. With the above mentioned properties and the low fabrication costs, polymers with electrical conductance would indeed be a technological marvel and this has led to a multidisciplinary effort, involving physical chemists, and materials and device scientists, since the early 1970's. Expectations have not been fully realized yet but the commercial use of polymeric solids as electrical materials is now

an established fact (Chapter 10). The semiconductive or metallic polymer notion has already been realized in polymers such as polyacetylene, including the ability to produce p or n type conductivity, though these materials as well as the phenomena clearly are still in the domain of research.

Experimental breakthrough was attained in obtaining flexible silvery films of $(CH)_x$ exhibiting semiconducting behavior. Further developments, through doping, led to increase of conductivity from the semiconductive to the metallic regime. Since then considerable information has been gathered on the various physical, chemical and structural properties of polyacetylene which has led to much needed insight into the topic of conducting polymers. Many intricate questions remain, though, including the nature of spinless charge carriers and the new concept of the mechanics of charge transport in organic systems. For example, due to the one-demensionality of an ideal $(CH)_x$ chain, many effects such as non-linearity, disorder and fluctuations are expected to be strongly enhanced. It is also assumed that bond alternation exists in polyacetylene but this has not been established in a satisfactory manner through experimentation. The number of reflections in electron or x-ray diffraction is still too low to determine the atomic positions in a PA crystal lattice. The question of bond alternation cannot be elucidated by infrared or Raman spectroscopy since the number of active modes is independent of the existance of bond alternation. Crystal lattice parameters for trans-polyacetylene are still controversial and at least three models have been proposed in this regard. Newest approaches to the delineation of the polymer structural features involve techniques including electron microscopy, x-ray scattering (low angle), small angle neutron scattering, vibrational spectroscopy and Mossbauer spectroscopy, among others.

REFERENCES

(1) M. Cohen, B.H. Kear, and R. Mehrabian, in "Rapid Solidification Processing: Principles and Technologies II", eds. R. Mehrabian, B.H. Kear, and M. Cohen, Claitor's Publishing Division, Baton Rouge, La., 1980, p. 1.
(2) J.T. Neil, *Materials Engineering*, March (1984) 37.
(3) L.M. Sheppard, *Materials Engineering*, April (1984) 36.
(4) W. Klement, R.H. Willens, and P. Duvez, *Nature*,*187* (1960) 869.
(5) P. Duwez and R.H. Willens, *Trans. AIME*, *227* (1963) 362.
(6) S.J. Savage and F.H. Froes, *J. of Metals*, *36*, April (1984) 20.
(7) E.J. Kubel, Jr., *Materials Engineering*, January (1984) 48.
(8) W.A. Grant, *J. Vac. Sci. Technol.*, *15 (5)* (1978) 1644.
(9) J.G. Wright, *Inst. Phys. Conf. Ser.*, *30* (1977) 251.
(10) J.C. Swartz, J.J. Hugh, R.F. Krause and R. Kossowksy, *J. Appl. Phys.*, *52* (1981) 1908.

(11) O.T. Inal, L. Keller, and F.G. Yost, *J. Mat. Sci., 15* (1980) 1947.
(12) O.T. Inal, C.V. Robino, L. Keller, F.G. Yost and M.M. Karnowsky, *J. Mat. Sci., 16* (1981) 3138.
(13) K.P. Mizgalski, O.T. Inal, F.G. Yost and M.M. Karnowsky, *J. Mat. Sci., 16* (1981) 3357.
(14) U. Koster and U. Herold, Proceedings of the Third Int. Conf. on Rapidly Quenched Metals, (1979) 281.
(15) P. Chaudary, B.C. Creissen and D. Turnbull, *Scientific American, 242 (4)* (1980) 110.
(16) L.E. Murr, O.T. Inal and S.H. Wang, *Mat. Sci. and Eng., 49* (1981) 57.
(17) O.T. Inal, L.E. Murr and F.G. Yost, *Mat. Sci. and Eng., 51* (1981) 101.
(18) O.T. Inal and W.F. Sommer, "Radiation Effects in Materials", in preparation (1984).
(19) R.D. McIntyre, *Materials Engineering*, February (1982) 34.
(20) Anonymous, *J. of Metals, 29* December (1977) 9.
(21) N.E. Paton and A.K. Ghosh, in "Metallurgical Treatises", eds. J.K. Tien and J.F. Elliot, AIME, 1981, p. 361.
(22) H.E. Chandler, *Metal Progress*, October (1981) 52.
(23) H.E. Chandler, *Metal Progress*, October (1982) 25.
(24) C.W. Chang and J. Szekely, *J. of Metals, 34*, February (1982) 57.
(25) K.J. Reid and P.J. Kaleka, *J. of Metals, 35*, December (1983) 30.
(26) K. Upadhya, J.J. Moore, and K.J. Reid, *J. of Metals, 36*, February (1984) 46.
(27) J.K. Hirvonen, *J. Vac. Sci. Technol., 15* (1978) 1662.
(28) W.A. Grant, *J. Vac. Sci. Technol., 15* (1978) 1664.
(29) W.E. Wood, *J. Mat. Sci., 18* (1983) 2555.
(30) O.T. Inal and C.V. Robino, *Thin Solid Films, 95* (1982) 195.
(31) C.V. Robino and O.T. Inal, *Mat. Sci. and Eng., 59* (1983) 79.
(32) B.H. Kear, J.W. Mayer, J.M. Poate, and P.R. Strutt, in "Metallurgical Treatises", eds. J.K. Tien and J.F. Elliott, AIME, 1981, p. 321.
(33) C.W. Draper, *J. of Metals, 34*, June (1982) 24.
(34) L.C. Chang and T.A. Read, *Trans. Met. Soc. AIME, 191* (1951) 47.
(35) W.J. Buehler and F.E. Wang, *Ocean Eng., 1* (1968) 105.
(36) L. McDonald Shetky, *Sci. Am., 24* (1979) 74.
(37) T.E. Johnson and A. Pocalyko,in "High Energy Rate Fabrication", eds. M.A. Meyers and J.W. Schroeder, ASME, New York, 1982, PVP-Vol. 70, p. 63.
(38) C.F. Cline and R.W. Hopper, *Scripta Met., 11* (1977) 1137.
(39) P.S. de Carli and J.C. Jamieson, *Science, 133* (1961) 1821.
(40) P.S. de Carli, "Method of Making Diamond", U.S. Patent 3,238,019, March 1, 1966.

(41) R.A. Graham, B. Morosin, and B. Dodson, "The Chemistry of Shock Compression: A Bibliography", Sandia Report SAND83-1887, October, 1983.

(42) T. Akashi, A. Sawaoka, and S. Saito, *J. Am. Cer. Soc., 61* (1978) 245.

(43) S. Saito and A. Sawaoka, Proc. 7th Intl. AIRAPT Conference, High Pressure Science and Technology, Le Crensot, France, 1979, p. 541.

(44) R.A. Graham, Sandia National Laboratories, Personal Communications (1984).

(45) A.B. Meinel and M.P. Meinel, "Applied Solar Energy", An Introduction", Addison-Wesley, N.Y. 1979 p. 295.

(46) A. Scherer, O.T. Inal and A.J. Singh, *Solar Energy Materials, 9* (1983) 139.

(47) R.J.H. Lin and P.B. Zimmer, "Optimization of Coatings for Flat-Plate Solar Collectors" Phase II, Honeywell Inc. Systems and Research Center, (1977) 85.

(48) O.T. Inal, M. Valayapetre, L.E. Murr and A.E. Torma, *Solar Energy Materials, 4* (1981) 333.

(49) B.D. Seraphin, "Spectrally Selective Surfaces and their Impact on Photothermal Energy Conversion", Solar Energy Conversion, Topics in Applied Physics, Vol. 31, ed. B.O. Seraphin, Springer Verlag, N.Y. (1976) 389.

(50) G. Zerlant, in "Critical Materials Problems in Energy Production", ed. C. Stein, Acad. Press, N.Y., p. 389.

(51) C.G. Crangvist and O. Hunderi, *J. Appl. Phys. 50* (1979) 1058.

(52) J.C. Mabon, O.T. Inal, and A.J. Singh, *Solar Energy Materials, 7* (1982) 359.